Constitutive law describing the phenomenology of subyield mechanically stimulated glasses

Luigi Grassia[†] and Alberto D'Amore[*]

Department of Aerospace and Mechanical Engineering, The Second University of Naples-SUN Via Roma 29, 81031 Aversa (CE), Italy

(Received 5 January 2006; revised manuscript received 10 March 2006; published 4 August 2006)

The principal features of the volumetric as well as the viscoelastic response of mechanically stimulated glasses can be summarized as follows: (i) the time-aging time shift factors contract upon increasing the probe stress (i.e., the stress apparently modifies the volume recovery kinetics), (ii) the volume recovery baseline remains unaltered (i.e., the underlying structure of the stimulated glass remains unchanged). Here we present a series of numerically simulated results concerning the responses of glassy polycarbonate that simultaneously fulfill these apparent contradictions. The problem was tackled coupling a modified Kalroush, Aklonis, Hotchinson, Ramos equation with the constitutive law for linear viscoelasticity within the domain of the reduced time. It was argued that the relaxation times under isobaric conditions depend on the temperature, the dimensionless volume, and the isotropic components of the stress tensor. Simulations are obtained with a minimum of experimental (*PVT* and linear viscoelastic) data inputs. Different loading protocols consisting of complex combinations and/or sequences of large and small mechanical stimuli were tested. Volumetric as well as viscoelastic behavior are systematically reported. A tentative explanation of the origin of the time-aging time contraction was finally proposed while some additional features concerning the volumetric response emerged.

DOI: 10.1103/PhysRevE.74.021504 PACS number(s): 64.70.Pf, 81.05.Lg, 83.60.Df, 82.35.Lr

I. INTRODUCTION

The simultaneous occurrence of structural relaxation and viscoelastic phenomena, referred to as *physical aging* [1–5], was the subject of a ponderous amount of literature data concerning the relaxation behavior of mechanically stimulated glassy materials. The main focus of the studies which appeared over the past quarter century is centered on the impact of mechanical stresses on the thermodynamic state of glassy materials [6–17]. Resolution of the problem is of great importance because it defines the level of complexity required to describe the mechanical response of glassy materials. If the mechanical perturbation alters the underlying structure of the glass, this must be accounted for explicitly in any constitutive law description of the behavior [18]. It is a matter of fact, however, that, due to the intricacy of the *physical aging* phenomenology, early studies were concentrated on simplified experimental and modeling strategies that can be described as follows: on one hand the amount of structural relaxation phenomena was accounted for by aging the samples in the absence of mechanical stresses; on the other hand the mechanical behavior of glassy polymers was obtained *suppressing* the effect of the ongoing structural relaxation during the experiments. Splitting the two phenomena was allowed in the following ways:

(i) The viscoelastic (as well as the ultimate properties) were measured at temperatures far below the glass transition temperature, T_g, after the glassy materials had experienced different thermal histories in the vicinity of the glass transition. It was assumed that the short-term tests were not influenced or negligibly influenced by the ongoing structural relaxation [19–22].

(ii) measurements at temperatures close to T_g, where the structural relaxation phenomena are highly activated, were performed following a simple (although arbitrary) procedure (referred to as protocol type I and detailed in the following), in order to overcome the thermorheological complexity emerging from materials that continuously change their structure [1]. The latter procedure was based on the concept of "momentary viscoelastic tests" and consists of the evaluation of viscoelastic properties within short time intervals, t_i, after the unloaded glass has experienced an (arbitrary) amount of structural relaxation subsequent to a quenching from above T_g to the test temperature. Under these circumstances the "*isostructural*" conditions were postulated by assuming that in the loading time interval the glass experienced an amount of structural relaxation that is negligible with respect to the relaxations accumulated previously.

Figure 1 shows the mechanical loading sequence (protocol type I) proposed by Struik to probe the viscoelastic response of a glass as structural recovery occurs [1]. Struik

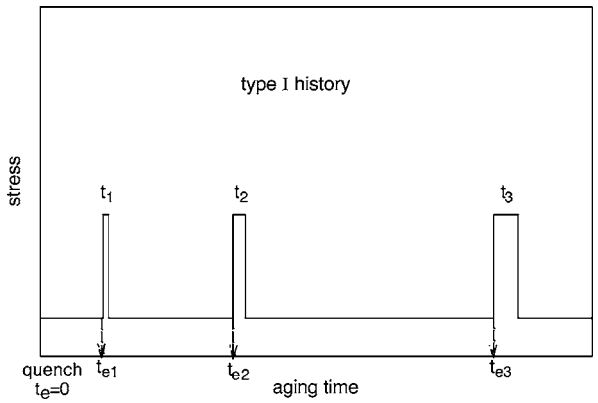

FIG. 1. Schematics of the protocol type I. The t_{ei} represent increasing aging times where $t_{ei} \propto 2t_{ei-1}$ $(i=1,2..)$. The t_i are the loading times and $t_i/t_{ei}=0.1$.

[†]Email address: luigi.grassia@unina2.it
[*]Email address: alberto.damore@unina2.it

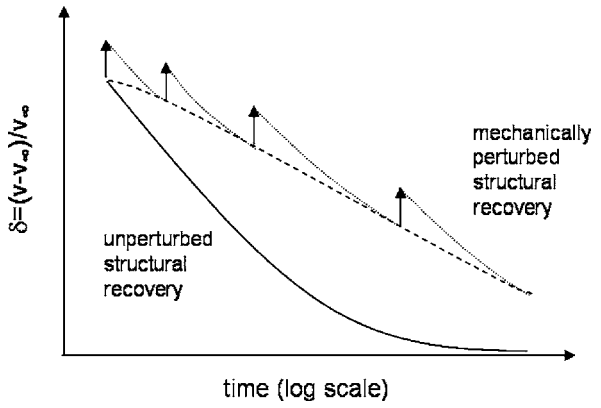

FIG. 2. Schematic of perturbed structural recovery expected to occur after large mechanical stimuli are applied to an aging glass according to the rejuvenation concept. (Adapted from Ref. [1].)

reported that time-aging time superposition applied to such responses and a "master" curve could be obtained allowing the definition of a time-aging time shift factor $a_{te}=\tau/\tau_{ref}$, where τ is the characteristic retardation time and τ_{ref} is the retardation reference time at a given elapsed time t_e^{ref} [1].

The time-aging time shift factor was reported obeying a power law function $a_{te}=At_e^{\mu}$ where the exponent $\mu=d\log a_{te}/d\log t_e$ is defined as the shift rate [1].

Struik always presented viscoelastic data held up by qualitative arguments supporting the idea that mechanical loading and volume recovery kinetics are mutually influenced [1]. In particular, he postulated a shift of the volume recovery baseline, qualitatively described in Fig. 2, due to the effects of the applied stresses and referred to as "*erasure of prior aging*," the effect of mechanical loadings. The idea was that, at a given temperature below T_g, "*severe*" mechanical stresses can reestablish partly or totally the initial (unaged) state of the glass in the same way as the erasure of prior aging is attained on glassy materials heated to above T_g and then quenched to below it (see Ref. [1], p. 88). To support this idea it was shown that upon increasing the level of stress the time-aging time shift factor decreases, as illustrated schematically in Fig. 3, i.e., the glass seems to recover part of the structural relaxation experienced previously [1]. The major effect is to reduce the (initial) slope, μ, of the $\log a_{te}$ versus $\log t_e$ plot, as illustrated in Fig. 4 for a commercial polycarbonate (LEXAN) tested at different stress levels.

It is worth mentioning that this sort of experiment was replicated for different polymers [10,11,15–17] (including thermosetting resins. In particular see Fig. 9 of Ref. [5]) and confirmed that at least in the power-law aging regime the result is unquestionable. Indeed, these kind of data were among the first taken as a signature of the mutual influence between mechanical loading and the glassy structure evolution. Later on, this effect has come to be referred to as *rejuvenation* [11].

A step ahead in the study of mechanically stimulated glasses is represented by the data published by McKenna and co-workers [13–15] concerning the simultaneous measurements of the volume recovery kinetics and the viscoelastic response. It was finally proved that, following the Struik protocol I, despite the presence of severe mechanical loadings

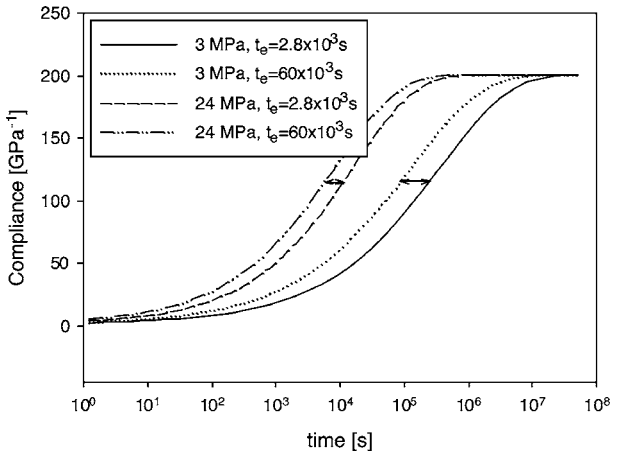

FIG. 3. Schematic of the impact of large stresses on the time-aging time shift factors. The creep compliance curves at small and large stress are derived from our modeling predictions.

(the protocol I consisted of torsional tests where both shear and normal stresses were in play) the volume recovery baseline (i.e., the volume relaxation behavior that one obtains in the absence of mechanical stimuli) remains unaltered. For the sake of clarity in Fig. 5 we report the results of our simulation (to be detailed in the following text) concerning the structural recovery for the unperturbed glass and for the sample loaded using the Struik protocol. Our model predicts that the volume recovery baseline does not change in the case of a tensile test.

Based on these unmistakable results it was argued that mechanical stress and volume recovery give rise to separable stress and volume relaxation phenomena. In few words, the time scales of mechanical and structural relaxation are somehow disconnected [18].

In a brief summary the two main (apparently contradictory) features of mechanically stimulated glassy materials (at least in the framework of protocol I) feeding the debate along the years, consist on the following unmistakable experimental evidence: (i) the time-aging time shift factor contracts upon increasing the probe stress (i.e., an apparent sample

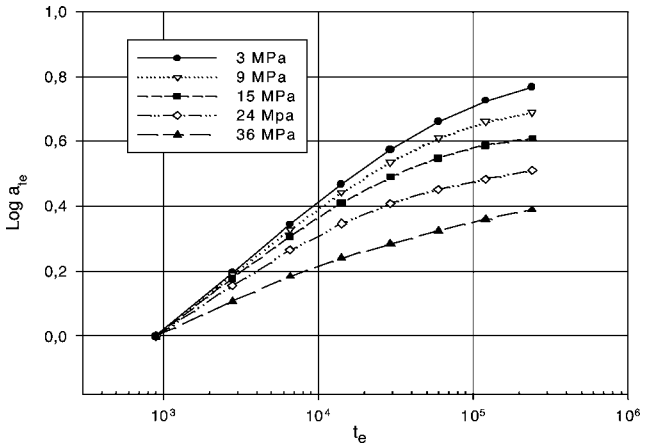

FIG. 4. Typical behavior of the shift factors vs the aging time for a polycarbonate (LEXAN) tested at different tensile stresses, as indicated markers: simulations, lines: guides for the eye).

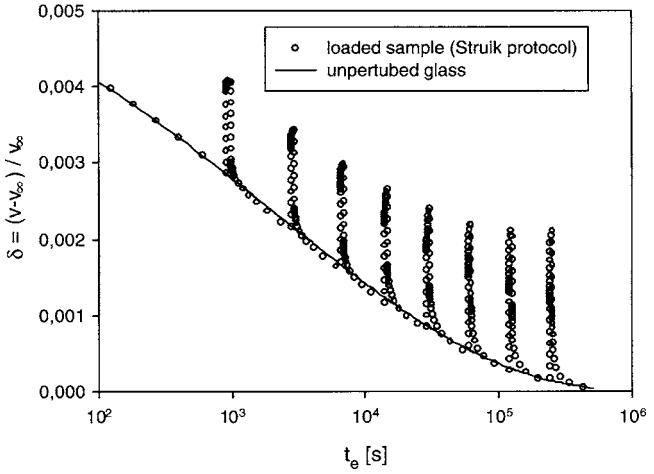

FIG. 5. Plot showing comparison of the structural recovery for the unperturbed glass (full curve) and for the sample loaded using the Struik protocol.

rejuvenation occurs). (ii) The volume recovery baseline is not affected by the mechanical loading (i.e., the underlying structure of the glass is not altered).

Currently, the following items remain open to scientific speculation: (a) the contraction of the time-aging time shift factors remain unexplained (b) the absence of a shift of the volume recovery baseline alone does not tell us anything about "rejuvenation" (incidentally, based on their qualitative arguments Struik and McKenna arrived at opposite conclusions [1,18,23]), (c) presently, the relevant available theories of mechanically stimulated glasses (referred to as "material clock models" in what follows) have not yet shown their capability to predict the experimental evidence (i) and (ii).

For these reasons the debate around *rejuvenation* produced other experimental methods (referred to as protocols II and III and detailed in the following) that differ essentially by the loading history (in both cases a combination and/or sequence of large and small mechanical stimuli). However, while protocol type I has the potential to settle the rejuvenation mechanisms in a straightforward way (by modulating the level of mechanical loading), the two remaining protocols result in a complex definition of adjunctive-nonstandard viscoelastic functions (in the case of protocol II) [10] and in a rather ineffective description of the results (in the case of protocol III) [1,15]. However, despite the above shortcomings, the complex loading histories derived from the application of the three protocols represent a formidable challenge for any law description of subyield mechanically stimulated glasses.

A substantial point emerged from the work of Simon *et al.* [24] even if in her work the loading conditions fall into the category of permanent subyield stimuli. It was shown that materials confined into nanosized pores age to a different state than that in the bulk. This was one of the rare examples of enthalpy relaxation measurements under isochoric conditions, where the relaxing hydrostatic tension under constant volume represents a "permanent," although transient, three-dimensional (3D) loading condition (this point will be treated during the discussion of protocol II which falls within the category of permanent loading histories). Further, it was suggested that the kinetics of glass-forming materials subject to different thermo-mechanical (*PVT*) paths may not be easily analyzed without a proper model of the interaction of the mechanical path and the structural relaxation path [25].

It should be added, for completeness, that, in the framework of the rejuvenation debate, some insights come from studies concerning the post-yield behavior of glassy polymers as the subyield behavior should, in some fashion, be related to the yield and post-yield behaviors. Hasan and Boyce [26] essentially showed that thermally and mechanically stimulated samples give rise to different glassy states. In their work, the enthalpy relaxation behavior of samples that had mechanically stimulated well above the yield stress was compared on the basis of the amount of resulting inelastic deformation. The essential points emerged can be summarized as follows: in sub-T_g annealed materials, the enthalpy overshoot at T_g decreases with inelastic strain until vanishing to some strain extent. At the same time both annealed and quenched materials show a pre-T_g exotherm (*absent in thermally rejuvenated samples*) evolving with the same trend until reaching a steady-state profile at some inelastic strain extent. A second post-T_g exotherm develops with further straining beyond such strain and is debited to the orientation-induced strain hardening of the material.

The above findings, together with other interesting speculations confirmed that yielding does not rejuvenate the glass, instead it may lead to a sort of polymorphism or new deformation induced phase [18]. In fact, Cangialosi *et al.* [27] showed that plastic deformation induces a dramatic change in the free volume microstructure, in terms of concentration and size of the free volume holes as measured by means of positron annihilation spectroscopy. The different free volume microstructure of plastically deformed glasses is far different from that of a thermally rejuvenated material and the subsequent physical aging, which is actually reinitiated, it has very different characteristics from that of a thermally rejuvenated sample. Further, molecular dynamic simulations within the potential energy landscape framework showed that plastically deformed glassy systems fall into a new minimum with different energetic and vibrational properties [28].

All the above considerations are somewhat in agreement with the general picture of Hasan and Boyce [26]: "*for small amount of strain (prior to yield) a small number of local transformations provides their isolation and results in rapid strain recovery upon unloading. With increasing strain beyond yield, however, the sites become more numerous and interact to produce relaxed configurations of a more long-range nature*."

Accordingly, yielding is a sort of turning point that allows sharing the phenomenology of mechanically stimulated glasses between subyield and post-yield behaviors. It is evident, however, that bridging the gap between the two behaviors represents a formidable task, that, at least to our knowledge, has been rarely attacked theoretically and not yet solved.

The reason is that we are still debating the impact of subyield mechanical stimuli on the evolving structure of a glass even in presence of the well established, irrefutable experimental features. On the contrary, from the point of

view of post-yield behavior serious contradictions emerged even within the same class of materials. For instance Broutman *et al.* [29] reported that polycarbonate and ABS undergo a decrease in density when subject to plastic deformation, while Cangialosi *et al.* [27] reported an increase in density for polycarbonate and polystyrene subjected to some amount of cold rolling and Van Melick *et al.* [30] showed that polystyrene maintains (or even slightly increases) its density after plastic deformation.

Finally, one should mention that from a different perspective the very existence of the yield stress (i.e., whether it is a myth or an engineering reality) has been questioned arguing that that "yield stress" is a *vanishing* concept as "*it seems likely that most, and perhaps all, materials will undergo flow at any stress since flow merely requires the existence of a relaxation mechanism*" [31–33]. In this paper we try to explain the warped phenomenology emerging from (subyield) mechanically stimulated glassy materials. Volumetric as well as viscoelastic behavior obtained under different loading protocols will be systematically reported. Some additional features concerning the volumetric response emerged that to our knowledge were never reported before. Based on general arguments, some small remarks from our simulations will indicate also a possible interpretation of the contradictory results emerging from the study on the post-yield behavior of glassy materials.

II. MODELING

There is a considerable body of literature that deals with the nonlinear viscoelasticity of glassy polymers that falls into the class of constitutive models that we refer to as "material clock models." The first ideas of material clocks go back to Leaderman in the 1940s [34] and the subsequent debates that ensued about the validity of time-temperature superposition in polymers, something especially stimulated when Williams, Landel, and Ferry [35] wrote their seminal paper on time-temperature superposition in 1955. Probably the best known model is the volume clock (or free volume clock) model of Knauss and Emri [36]. More recently, Lustig, Shay, and Caruthers [37] and Caruthers, Adolf, and Chambers [38,39] have carried out extensive analyses of rational mechanics based nonlinear thermodynamics that they claim can do structural recovery and nonlinear viscoelasticity. Their approach is based on internal energy and appears of very general interest. However, the above mentioned theories do not address the phenomenology of mechanically stimulated glasses directly, at least in light of the predictions of the substantial features discussed in the introduction that have been feeding the debate along the years.

To that end, the capability of these models to predict of the main features of mechanically stimulated glasses remains unknown to the present authors. It is a matter of fact, however, that when the simultaneous volume and stress relaxation phenomena are of concern a model coupling the two phenomena is required. This simple concept was the basis of our modeling strategy that, basically, provides a stress clock addition to the phenomenology of structural relaxation.

A. Development of the theory

Our approach derives from the well established phenomenological theories capable of capturing the principal features (nonlinearity and memory effect) of structural relaxation. In this respect both KAHR (Kalroush, Aklonis, Hutchinson, Ramos) [40,41] and TNM (Tool-Narayanaswamy-Moynihan) [42–44] theories predict with accuracy the *PVT* curves of any glass forming material. Indeed, despite the fact that the parameters of KAHR and TNM theories are strongly correlated (their use is really equivalent under isobaric conditions) the KAHR theory accounts explicitly for the (external) pressure and represents a more viable formalism for our purposes. For completeness, while it is certainly true that the empirical parameters in KAHR theory suffer some lack of physical meaning (due to the arbitrary dependence of relaxation time on temperature, pressure, and dimensionless volume), the general *PVT* (pressure, volume, temperature) behavior, under arbitrary temperature and/or pressure histories, can be suitably predicted with a single set of parameters. However, TNM and KAHR theories are widely used to study the *intrinsic* phenomenology of structural recovery. To do this, small pieces of materials are utilized in apparatus like DSC or mercury dilatometer (for the purpose of studying the enthalpy and the volume relaxation kinetics, respectively) where uniform conditions (within the sample) are postulated to be achieved in a way that the programmed inputs (in terms of pressure and/or temperature histories) are considered coincident with those suffered by the sample. This is not the situation when materials with finite dimensions are under concern. Under the latter circumstances the available phenomenological theories of the glassy state do not contain the essential *ingredients* to follow the volume and/or enthalpy recovery kinetics at each body point. For instance, when dealing with dilatometric experiments on objects of finite size, one measures the overall volume variations (under given thermal histories) as a sum of the individual contributions of each body point. However, the individual points are subjected to different stimuli (caused by transient heat transfer phenomena) that give rise to different structural relaxation kinetics. Since the individual points are not separated (the congruence equation is the mathematical formalism that physically linked the points) the differential volume variation between adjacent points gives rise to the mechanical interaction that represents the source of local stress buildup. The stress field, however, can be resolved once the force balance equations are imposed. Under isothermal conditions mechanically stimulated materials give rise to the same kind of considerations. Arbitrary mechanical loadings would produce different volumetric effects on the individual (yet not separated) body points. Locally, the time dependent volume variations due to the mechanical stress are debited to the isotropic part of the stress tensor through the "local" bulk relaxation modulus. At the same time the volume perturbations-induced stresses give rise to a modification of the structural relaxation kinetics.

To better clarify, in Figs. 6 and 7 the background of the phenomenology is illustrated: in bodies of finite size the volume recovery behavior at a point becomes perturbed by the additional effect of the local isotropic part of the stress tensor

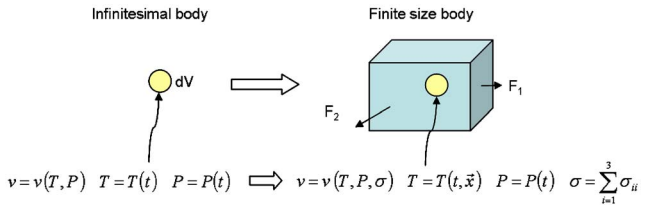

FIG. 6. (Color online) Schematic of the scaling effects from "small" to finite size body. $\vec{x}$ is the geometrical position.

originated by the external perturbations (F_1,F_2). This aspect is geometrically described in Fig. 7, where the effect of the mechanical stress at a given point, in terms of volume departure from equilibrium, δ, and fictive temperature, T_f, is reported conforming with the KAHR and TNM variables, respectively.

Following this discussion we assume that in presence of a stress field the structural recovery is described by a modified KAHR formalism assuming that the isotropic part of the stress tensor plays the same role of the external pressure.

Replacing the pressure with the spherical part of the stress tensor in the KAHR equation renders an immediate constitutive link between the structural relaxation kinetics and the mechanical behavior of a finite size body. Therefore the KAHR model is modified as follows:

$$\delta^f = \frac{v - v_\infty^f}{v_\infty^f} = \int_0^\xi \left(-\Delta\alpha \frac{dT}{d\xi'} - \frac{1}{3}\Delta k \frac{d\sigma}{d\xi'} \right) M(\xi')d\xi', \quad (1)$$

where δ^f is the dimensionless volume with respect to the equilibrium fictive volume, v_∞^f (defined below), T is the temperature, $\sigma=\Sigma_{i=1}^3\sigma_{ii}$ the isotropic part of the stress tensor, $\Delta\alpha=\alpha_\infty-\alpha_0$ and $\Delta k=k_\infty-k_0$ with α_∞, k_∞ and α_0, k_0 being the thermal expansion and the isothermal compressibility coefficients in the liquid, l, and in the glassy, g, state, respectively $\left(\alpha_\infty=\frac{1}{v}\left(\frac{\partial v}{\partial T}\right)_l, \alpha_0=\frac{1}{v}\left(\frac{\partial v}{\partial T}\right)_g, k_\infty=\frac{1}{v}\left(\frac{\partial v}{\partial P}\right)_l, k_0=\frac{1}{v}\left(\frac{\partial v}{\partial T}\right)_g\right)$. ξ is the reduced time defined as follows:

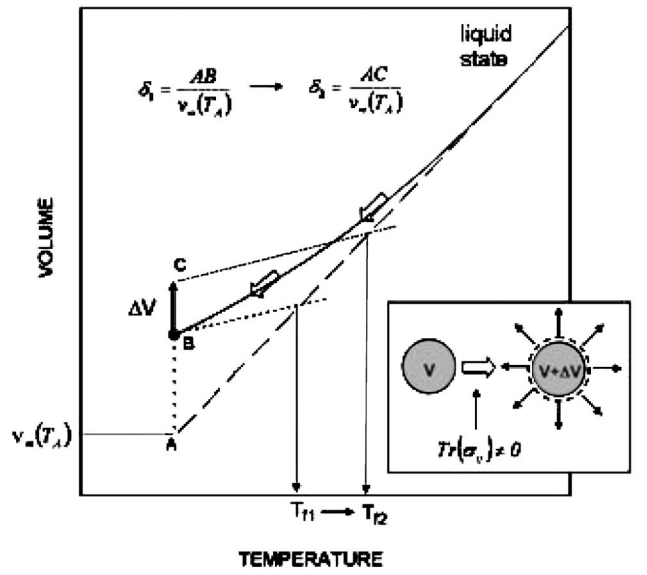

FIG. 7. The geometric description of the effect of the isotropic part of the stress tensor on volume relaxation. The arrows indicate the specific thermal history at a given point within the body.

$$\xi = \int_0^t \frac{dt'}{a_T a_\sigma a_\delta}, \quad (2)$$

where a_T, a_σ, a_δ, are the shift factors describing the dependence of structural relaxation times on temperature, mechanical stress and structure, and

$$M(\xi) = \exp\left[-\left(\frac{\xi}{\tau_r} \right)^\beta \right] \quad (3)$$

is the memory function expressed by the stretched exponential. β is the shape parameter and t_r the characteristic relaxation time at a reference temperature.

The fictive volume v_∞^f, appearing in Eq. (1), takes the following form as it depends on both the temperature and loading condition:

$$v_\infty^f = \alpha_\infty(T - T_0) + \frac{1}{3}k_\infty(\sigma - \sigma_0) + v_\infty^0, \quad (4)$$

where T_0 is the initial temperature, σ_0 the preexisting (residual) stress (presently it is assumed $\sigma_0=0$), and v_∞^0 the initial volume.

The shift factors appearing in the expression of the reduced time, ξ, fulfill the simplest form as possible, i.e., the logarithmic of the relaxation time depends linearly on the temperature, the isotropic part of the stress tensor and the dimensionless volume. Their explicit expressions are:

$$a_T = \exp[-\theta_T(T - T_{ref})], \quad (5)$$

$$a_\sigma = \exp[-\theta_\sigma(\sigma - \sigma_{ref})], \quad (6)$$

$$a_\delta = \exp\left[-(1-x)\delta\left(\frac{\theta_\sigma}{\Delta k} + \frac{\theta_T}{\Delta\alpha} \right) \right]. \quad (7)$$

Equation (5) and (6) are identical to those utilized in the framework of KAHR theory except that the pressure is replaced by σ. θ_T and θ_σ are material constants. The structure-dependent shift factor is expressed by Eq. (7) and contains the nonlinearly fitting parameter $x(0<x<1)$: if $x=1$ the volume dependence of relaxation times vanishes and the nonlinearity falls out. The symbol δ appearing in the expression of a_δ is the dimensionless volume calculated according to

$$\delta = \frac{v - v_\infty}{v_\infty}, \quad (8)$$

where v_∞ is the equilibrium volume under isobaric conditions.

Equations (5)–(7) do not account for the deviatoric part of the stress tensor according to the findings of Ref. [6] where it was concluded that "*the mean normal strain and not the octahedral shear strain is the principal factor that governs both the effect of strain field on relaxation kinetics and the onset of the nonlinear viscoelastic behavior.*"

To a first approximation we assume a linear dependence of the equilibrium volume on temperature, so that its expression is

$$v_\infty = \alpha_\infty (T - T_0) + v_\infty^0. \tag{9}$$

The linear dependences expressed through Eqs. (5)–(7) represent valid approximations when a narrow range of temperature is of concern.

In order to numerically solve Eq. (1) one needs to couple it with a material constitutive equation establishing the relationship between stress and strain. We will use the formalism of the constitutive equation for linear viscoelastic material behavior within the domain of reduced time (defined above):

$$\sigma_{ij} = \delta_{ij} \int_0^\xi B(\xi - \xi') \frac{d}{d\xi'} (\varepsilon - \theta) d\xi' + \int_0^\xi G(\xi - \xi') \frac{d}{d\xi'} \left(\varepsilon_{ij} - \frac{1}{3} \delta_{ij} \varepsilon \right) d\xi', \tag{10}$$

where B and G are the bulk the shear relaxation moduli $\varepsilon = \Sigma_{i=1}^3 \varepsilon_{ii}$ and θ are the free deformation due to the thermal effects. Shear and bulk moduli are assumed to obey the following functional forms:

$$B(\xi) = \frac{1}{k_0} + \left(\frac{1}{k_\infty} - \frac{1}{k_0} \right) \left(1 - \exp\left[- \left(\frac{\xi}{\tau'_{ref}} \right)^{\beta'} \right] \right), \tag{11}$$

$$G(\xi) = G_0 + (G_\infty - G_0) \left(1 - \exp\left[- \left(\frac{\xi}{\tau''_{ref}} \right)^{\beta''} \right] \right), \tag{12}$$

where τ'_{ref} and τ''_{ref} are the mean bulk and shear relaxation times at a reference temperature, respectively.

The thermal free deformation is given by:

$$\theta = \frac{v_f - v_0}{v_0}, \tag{13}$$

where v_o is the volume at the start of the loading history. The dimensionless free deformation, θ, can be calculated through v_f, according to the KHAR model taking into account the thermal effects alone as follows:

$$\frac{v_f - v_\infty}{v_\infty} = \int_0^t \left(- \Delta\alpha \frac{dT}{dt'} \right) \exp\left[- \left(\int_{t'}^t \frac{dt''}{\tau_r a_T a_\sigma a_\delta} \right)^\beta \right] dt'. \tag{14}$$

Concerning the bulk relaxation function, B, appearing in Eq. (11), we argue that the memory function, $M(\xi)$, coincides with the dimensionless bulk compliance in the reduced time domain, i.e.:

$$\frac{C_\infty - C(\xi)}{C_\infty - C_0} = M(\xi), \tag{15}$$

where $C(\xi)$ is the bulk compliance, C_∞ and C_0 the relaxed and unrelaxed bulk compliances that coincide with k_∞ and k_o respectively (see below for the details of such an assumption). So that the parameters t_r and β appearing in Eqs. (3) and (11) are related by means of the Laplace transform, in the Laplace domain the relationship between the memory function and the bulk relaxation modulus is given by:

$$\frac{C_\infty}{s} - [C_\infty - C_0] M^*(s) = \frac{1}{s^2 B^*(s)}, \tag{16}$$

where s is the complex variable in the Laplace domain and M^* and B^* are the Laplace transforms of M and B, respectively.

B. Some remarks about the modeling strategy

From our modeling approach it comes out that only two experimental data sets (namely, the *PVT* and the "equilibrium" shear relaxation data) are required to numerically solve the integral Eqs. (1) and (10).

We point out that most of the parameters which appear in Eqs. (1)–(16) come directly from the experimental data while the fitting parameters are reduced to a minimum, as can be appreciated in the following: (i) From Eq. (11) it can be observed that the relaxed and unrelaxed bulk moduli have been assumed equal to the reciprocal of the isothermal compressibility coefficient in the liquid and the glassy state, respectively. However, while in the liquid state the bulk modulus, B, and the reciprocal compressibility, k, coincide, this is not true in the glassy state since the system is out of equilibrium. The same arguments hold true when the shear relaxation modulus, G, and the coefficient of thermal expansion, a, are of concern. It is assumed, however, that the unrelaxed parameters, k_0, G_0, α_0 and the relaxations strength, Δk, ΔG, Δa, remain invariant on aging. However, since our approach is confined to a narrow range of temperature close to T_g, these approximations result in are quite small error. (ii) The thermal expansion and the isothermal compressibility values in the liquid and in the glassy state (α_∞, α_0 and k_∞, k_0) and the limiting shear moduli (G_0, G_∞) derive directly from the experimental *PVT* and viscoelastic data, respectively. (iii) The shear modulus master curve was modeled with the stretched exponential function with parameters t''_{ref} and β'' obtained by least square methods. (iv) The KAHR parameters (t_{ref}, β, x, θ_σ, and θ_T) are obtained by least square nonlinear optimization fitting procedure.

In addition, based on the *PVT* data the parameters θ_σ and θ_T can be extracted directly from the measured temperature and pressure T_g dependence, and (eventually) used as tentative input data within the optimization procedure of the KAHR parameter. In such a way the optimum set of parameters succeed very rapidly. Incidentally the calculated values of θ_σ and θ_T are practically coincident with those obtained directly from the experimental *PVT* data. Then the KAHR parameters reduce substantially to only three (t_{ref}, x, and β) if one recognizes the equivalence reported above, the remaining data input being measured quantities.

The calculated sets of structural and viscoelastic relaxation parameters remain fixed once and for all, while the numerical simulations claim only for the thermal and/or the loading histories input data.

Finally, while the formalism utilized for the shift factors is unable to describe the observed Williams, Landel, and Ferry (WLF) [35] temperature dependence in the equilibrium limit,

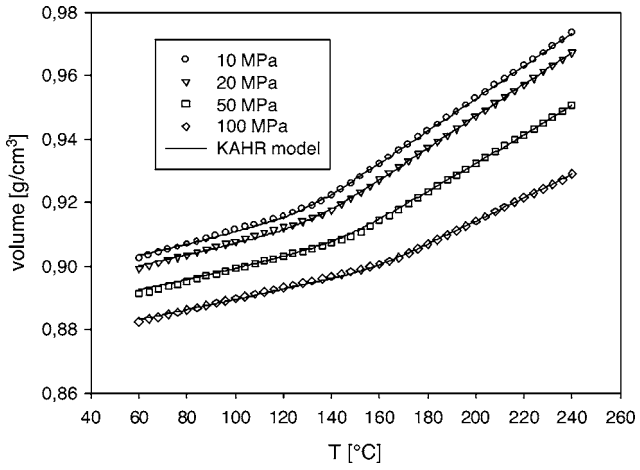

FIG. 8. Polycarbonate *PVT* data (symbols) and predictions based on KAHR theory (solid lines).

it is often thought to be a valid approximation to the narrow range of temperatures over which data are obtained and modeled.

III. EXPERIMENTAL DATA

Figures 8 and 9 illustrate the typical *PVT* and the linear viscoelastic data for a commercially available polycarbonate (LEXAN, GE Company) used as test material (T_g=142°—calorimetrically determined, M_w=30 900, M_n =19 700, PDI=1.57).

Dilatometric study was performed by using a pressure-volume-temperature (*PVT*) apparatus by GNOMIX. The data in terms of volume change were obtained at the cooling rate of 1 °C/min. Volume changes were normalized to the absolute values by measuring the room temperature density of polycarbonate by a density column gradient.

The KAHR parameters, [θ_T=0.51 θ_σ=0.17 x=0.69 β =0.44 ln(τ_r)=7.2, with T_{ref}=416 K] have been calculated through a nonlinear best fit procedure and remain fixed once and for all in our numerical simulation. As expected the KAHR theory gives rise to excellent curve predictions (dotted lines) of the *PVT* data. The stress relaxation experiments were carried out on a Rheometrics-Ares viscoelastic analyzer. Samples in the form of rectangular sheets of 25×8 ×2 mm^3 were utilized. The shear relaxation modulus in the form of a master curve at a reference temperature of 142 °C was obtained via the time temperature superposition procedure by shifting the data obtained in a narrow temperature interval (from 135 to 155 °C) above the glass transition temperature. In spite of the fact that the data at 135 °C fall somewhat below T_g, they served uniquely to control the consistency of the glassy plateau estimate obtained at higher temperature.

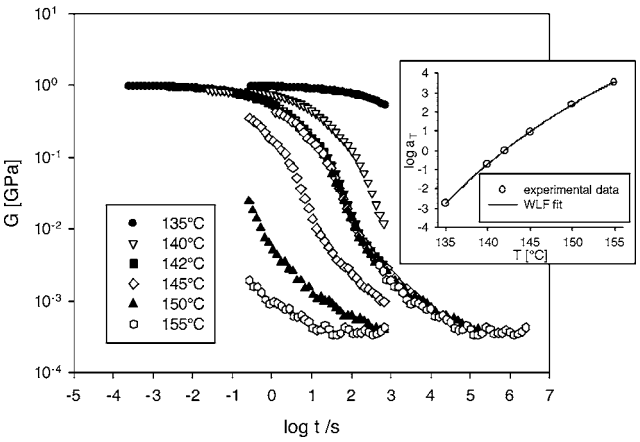

FIG. 9. The shear relaxation modulus "master curve" for polycarbonate and the corresponding shift factors (insert) (T_{ref}=142 °C).

The viscoelastic data were numerically manipulated by using a generalized Maxwell model. When using the stretched exponential function they resulted in a shape parameter β''=0.438 and a characteristic relaxation time t_r'' =3.57 s.

IV. RESULTS AND DISCUSSION

A. Numerical simulations premise

Before analyzing the results of our modeling approach let us recall that, in a previous work based on TNM theory, D'Amore *et al.* [45,46] showed that substantial residual stresses can arise in unloaded polymeric objects (in the form of slabs and cylinders), quenched from above to below T_g. In their work, with the aid of finite element analysis, they developed a numerical routine accounting for the different volume relaxation kinetics at each body point resulting from the transient heat transfer phenomena. Depending on the Biot number (i.e., the combination of the relevant dimensions of the object and the heat exchange efficiency) and the degree of under-cooling ($T-T_g$), residual stresses, varying from negative to positive values along the samples thickness, were calculated. Accordingly, density and fictive temperature gradients appeared as well. For the purpose of using the *clean* mechanical histories of protocol I, II, and III, in this work we will replicate the viscoelastic and volume recovery data that appeared in the literature accounting only for the applied nominal loading history, in spite of the fact that the amount of error resulting from disregarding the residual stresses can be numerically evaluated. The reason is that taking into account the residual stresses would inevitably compel a distortion of the local effective stresses along the sample thickness with respect to the external applied stress (actually representing the input function in our modeling). Assuming uniform loading conditions help the numerical simulations much faster. At the same time, we are confident that even disregarding the residual stresses at temperatures close to T_g (where they are considerably relaxed) the overall physics underlying the phenomenology is not lost.

B. Protocol I

The simulation starts assuming a rapid quench from T_g +20 K down to T_g−20 K and holding the temperature constant. Following protocol type I of Fig. 1 the sample was then subject to five different levels of tensile stress, ranging

from 3 to 36 MPa. The data in term of dimensionless volume are reported in Fig. 5 for a tensile stress of 15 MPa. Commenting on Fig. 5 is straightforward: constitutively coupling the structural and the viscoelastic relaxation phenomena one can predict that the volume recovery baseline remains unaltered (for completeness the simulations showed the same behavior at each level of stress). These results are consistent with the general features reported in Ref. [13] and, at first glance, with the Struik speculations supporting the rejuvenation that appeared [23] in a comment to the data of Ref. [13].

In Fig. 4 the shift factor as function of aging time is reported for the five different loading conditions. It is worth noting that our model predicts that the shift rate, μ, decreases as the stress increases and eventually levels off at longer times as reported in Refs. [11,16]. More importantly, it comes out that the shift rate levels off as equilibrium is approached (see the time scale to the approach of equilibrium in Fig. 5 for comparison).

However, since the discussion converges invariably on the concept of rejuvenation we try to contribute with the following series of arguments.

C. Volume recovery baseline

As mentioned before, upon coupling the viscoelastic and structural relaxation, our model predicts that the volume recovery baseline remains unaltered while this result was taken as proof that stress and structure are somewhat separated. These arguments would tend to admit rejuvenation, at first glance. Instead, what can be surely affirmed is that (in the subyield region) mechanical stresses alter the "momentary" underlying structure of the glass that, in fact, recovers its baseline as soon as, upon unloading, the stress is relaxed. McKenna, based on his outstanding results, pointed out that mechanical perturbations do not influence the thermodynamic state of the glass. This comes to be true in the light of subyield momentary stimuli (short-term mechanical perturbations). Under the circumstance of a permanent stress and/or deformation, the volume recovery kinetics is *permanently* affected giving rise to a different relaxation behavior when compared with that of the (unperturbed) bulk material. This is exactly the case illustrated in Ref. [24], already discussed, where changes in the structural recovery kinetics were demonstrated by means of enthalpy relaxation measurements.

D. Stress-induced shift factors contraction

Despite the above argumentations, the real signature of rejuvenation was attributed to the shift factors contraction illustrated in Fig. 4. Explaining the origin of the shift factors contraction is not trivial while doing it will end one of the main chapters of the glassy state. Our arguments about the matter are supported by a close inspection of Figs. 10 and 11, where the same kind of results illustrated in Figs. 4 and 5 are reported at two different stress levels (we selected 3 and 24 MPa to give rise to a better resolution about the focus of our discussion) and can be summarized as follows: we recall that in the framework of protocol I, where the temperature

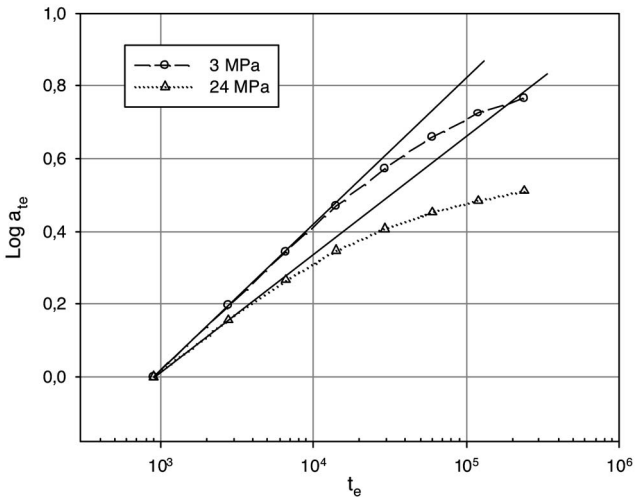

FIG. 10. The time-aging time shift factors at different stresses. The two straight lines are drawn to illustrate the departure from the power-law region that, actually, is anticipated at higher stresses (markers: simulations, lines: guides to the eye).

and the stress are fixed, the "dimensionless volume" (i.e., the structural parameter) during the tests is uniquely responsible for the retardation time difference between adjacent creep tests. Based on this argument, one can readily see that by linking the peaks of the volumetric creep response at each stress level (roughly illustrated by the dotted lines) the resulting (although arbitrary) curves show flatter slopes at higher stresses corresponding to lower shift factors (see Fig. 10 for comparison). Linking the volume recovery peaks makes sense now: it allows a rapid (and rough) estimation of the volume creep extent with respect to the volume recovery baseline.

In addition, at a given stress, one can appreciate that, as long as the time elapses, flattening proceeds (and eventually levels off) until the undisturbed volume recovery baseline approaches equilibrium, where the time-aging time shift factors level off (these same features can be noticed in the original experimental data which appeared in Refs. [10,12,15]).

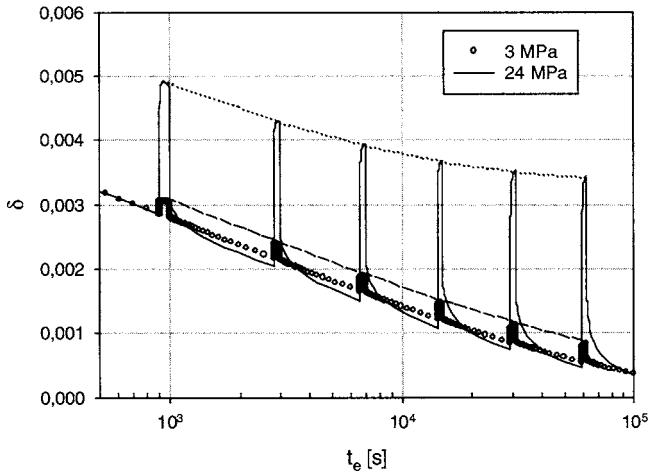

FIG. 11. Simulated volume recovery data under two different loading conditions.

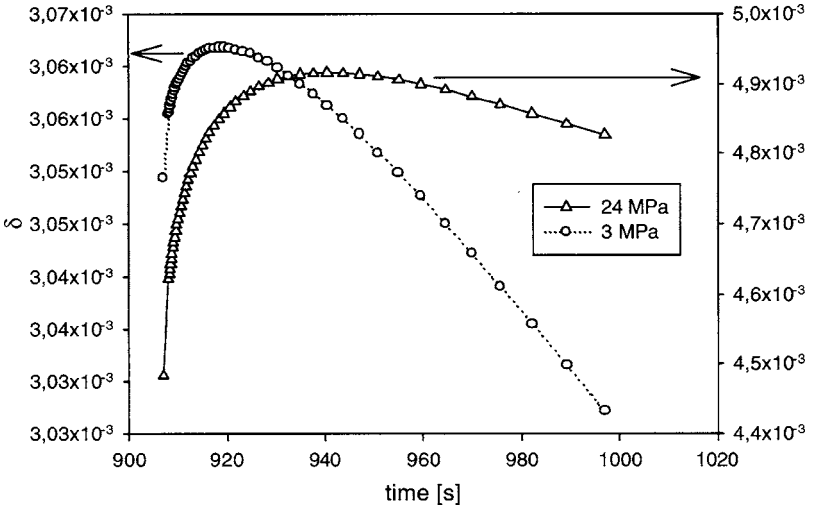

FIG. 12. Volume creep behavior at the start of the loading history. For clarity the instantaneous (elastic) responses upon loading and unloading are not reported (markers: simulations, lines: guide to the eyes).

Why the curves linking the volume recovery peaks flatten at higher stresses and longer times is the argument that follows.

First of all the overall creep extent is the combination of two direct effects: one is the inherent volume recovery originated by the glass instability that leads to a volume contraction after down quenching, the other is the effect of the isotropic part of the stress tensor that, during tensile loadings experiments, implies dilitation (by way of the bulk creep compliance). At longer elapsed times the underlying driving force for volume recovery tends to vanish, actually, resulting in a lesser (negative) contribution to the overall volumetric creep extent, while higher stresses implies larger dilatations. Accordingly, comparing two adjacent volume creep curves at different stress levels (see Fig. 11) it is evident that the volume creep responses show lesser differences at higher stresses due to three main reasons:

(i) the extent of the underlying volume relaxation (i.e., the baseline) contribution is irrespective of the actual stress,

(ii) the contribution of the isotropic part of the stress tensor increases (increasing the actual volume) with the stress, and

(iii) the volume creep rate (depending on the actual volume) is faster.

Claiming again Fig. 3, the dramatic effect of the above statements can be readily appreciated, i.e., at higher stress the glass softens and shows steeper creep compliance behavior leading to the expected shift factor contraction.

E. Stress and structure interplay

To illustrate dramatically the counteracting volume relaxation and the stress-induced volume effects, in Fig. 12 we report on the volume creep behavior for two different levels of stress at the start of the loading sequence, where the glass stands very far from equilibrium. The two behaviors appear quite similar: the dimensionless volume, δ, shows in both cases a nonmonotonous creep behavior and exhibits a maximum. In particular, at higher stresses the curve maximum shifts to longer times, conforming to the fact that the enhanced creep extent requires a wider volume relaxation contribution (that, irrespective of the actual stress, is reached at longer times) to be counterbalanced. From a close inspection of Fig. 11 it can be readily seen that as the aging time elapses the underlying volume relaxation contribution tends to vanish so that upon loading the volume creep responses show monotonic behaviors. Indeed, at longer times the creep curves become steeper as stated above.

Furthermore, inspecting Fig. 11 with reference to the higher stress, it appears clearly that, upon unloading, the volume relaxes beneath the volume recovery baseline and eventually recovers again its baseline as expected (see also Fig. 5 of Ref. [12]). Such undershoots show increasing strength at shorter times and appear minimal at the lower stress. In fact, unloading corresponds to the application of a negative probe stress that gives rise to mechanical relaxations occurring in the same direction of the (negative) contribution of the underlying structural relaxation. From these arguments one can appreciate that the volume recovery undershoots tend to vanish at longer times and are minimized at lower stresses. Concerning the shift rate, μ, it reflects the time-aging time shift factors behavior. It is worth mentioning however, that the response of the time-aging time shift factors should be sigmoidal with the power-law dependence being what is observed in experiments carried out in a limited aging time window. At any rate, the short time end of the response is not readily accessible by experiments. Actually, in the framework of protocol I the time elapsed before the start of the loading history cuts off the short time end of the sigmoidal response. Accordingly, starting from the intermediate region the shift rate is in all cases a monotonic decreasing function of the aging time conforming to the downward curvature of the time-aging time shift factors reported in Fig. 9 of Ref. [15] as well as in Fig. 4 concerning our predictions. It is worth noting that in the relevant paper by Caruthers [39] the prediction of the time-aging time shift factors was also attempted. However, neither the downward curvature nor the shift factors leveling off was reported.

F. Primitive considerations on post-yield behavior

The results illustrated in Fig. 12 allow an additional consideration of general interest. As mentioned before, it is fre-

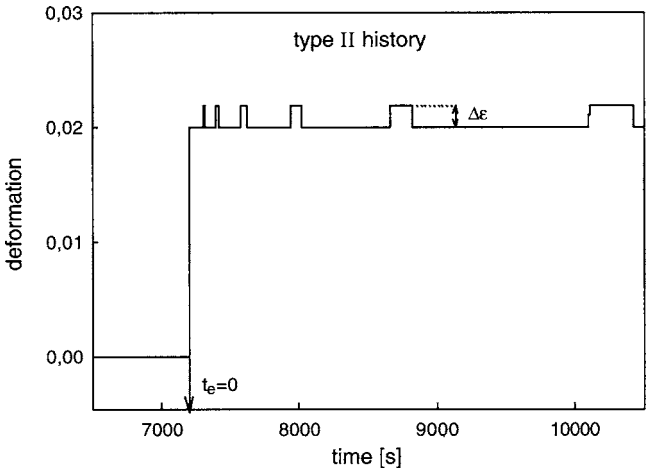

FIG. 13. Schematic of the protocol type II.

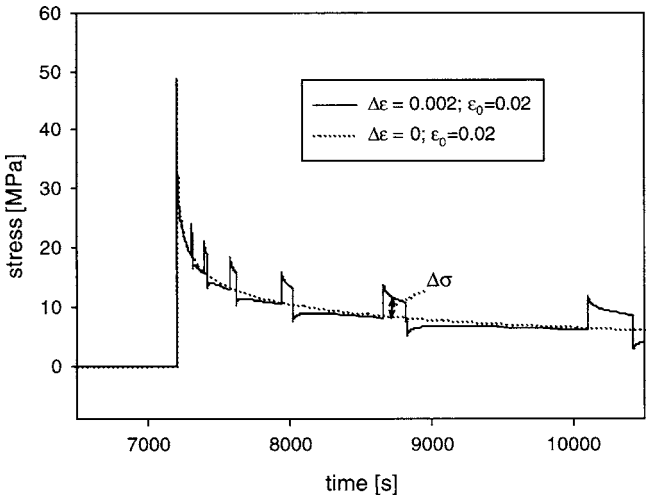

FIG. 14. Simulated axial stress response during the protocol type 2: solid line $\Delta\varepsilon=0.002$; dotted line $\Delta\varepsilon=0$.

quently reported [27,29,30] that "severe" mechanical stresses beyond the yield stress can produce both matter densification and dilatation. It is clear, now, that the two occurrences can be simultaneously true depending on the proper time scale adopted. In fact, post-yield mechanically stimulated glasses attain a different glass structure [18,26–28] but, actually, aging is reinitiated and eventually proceeds with different kinetics with respect to the bulk. However, aging can reinitiate (then the volume relaxes towards its new equilibrium value) before eventually the mechanical loading is ended. Therefore, depending on the time scales and the relative importance of the structural and the stress-induced volume relaxation, the glass can decrease, maintain or increase its density after plastic deformation.

V. PROTOCOL TYPE II AND III

Two other different protocols are utilized in the literature for the sake of demonstrating the existence of rejuvenation. In this section we report on the results of our simulations concerning protocols type II and III. According to these protocols the glass is subjected to a combination of large and small mechanical stimuli. Figure 13 illustrates the protocol type II. Here a "small" strain, $\Delta\varepsilon=0.1\varepsilon_0$, is superimposed (according to the protocol type I) to a large constant strain $\varepsilon_0=0.02$.

The results are generally reported in terms of incremental viscoelastic function as follows [9,10,15]:

$$\Delta E = \frac{\Delta\sigma(t)}{\Delta\varepsilon},$$

where ΔE is the incremental modulus, t is the time after imposition of the small probe strain $\Delta\varepsilon$, and $\Delta\sigma$ is the incremental stress response. Figure 14 show the results of our simulation in terms of the overall stress relaxation response while in Fig. 15 the data are reported in terms of ΔE [9,10,15] as a function of aging time. According to the results reported in the literature [10,12] two essential features emerge: (i) one can observe that ΔE curves shift toward shorter times with respect to the linear viscoelastic response (it is reported that the glass "softens" due to the large strain) and (ii) upon increasing the elapsed time ΔE curves tend toward the "linear" viscoelastic response (it seems that aging is reinitiated due to the impact of large mechanical stimuli).

In addition it can be argued that the magnitude of these effects increase as the applied deformation increases. McKenna and Zapas [12] used a nonlinear constitutive equation to address the interpretation of the above results. In fact, the model overestimates *the glass softening* and allows a qualitative description of the observed phenomena as reported in Fig. 7 of Ref. [10].

A different explanation of these phenomena can be given by looking at the corresponding results in terms of volume recovery behavior (never reported before) as illustrated in Fig. 16. Softening with respect to the linear case is due to the higher dimensionless volume (higher mobility) resulting from the large deformation. Practically the volume recovery resulting from the large (permanent) deformation represents the baseline to which the response of the small probes rely on. As long as the time elapses the volume relaxation due to the large probe reduces the strain softening effect. So that the

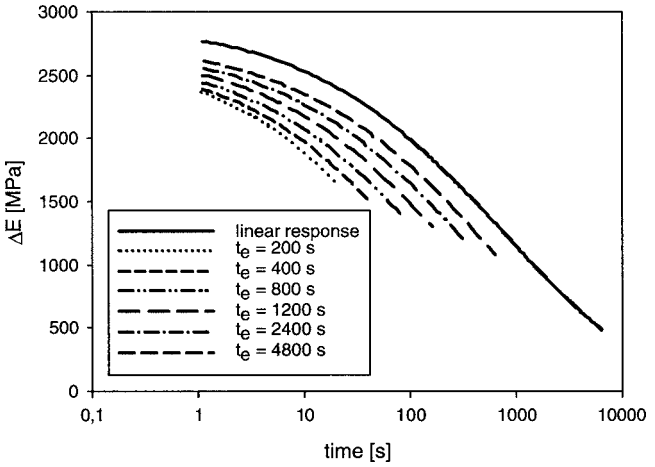

FIG. 15. Simulated incremental relaxation modulus during aging.

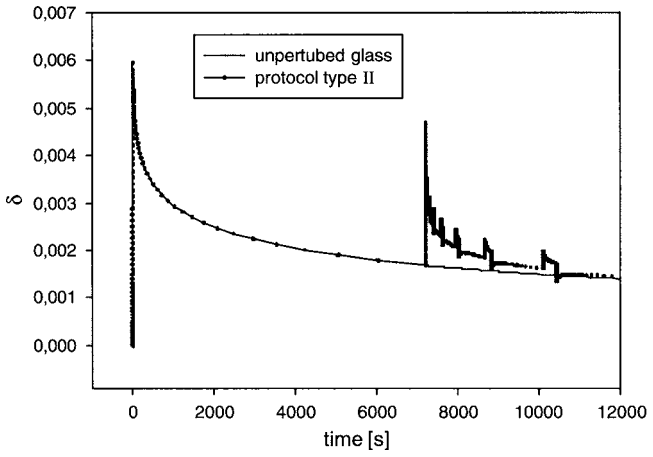

FIG. 16. Plot showing comparison of the simulated structural recovery for the unperturbed glass (full curve) and for the sample loaded using the protocol II.

stress relaxation curves shift toward the linear response. Therefore, items (i) and (ii) are a manifestation of the same phenomenon. One should recognize that it is the interaction between the large mechanical impulses and the underlying structure (the thermodynamic state) of the glass that momentarily governs the viscoelastic as well as the structural relaxation response.

It is evident that the relaxation behavior at each step of the superposed protocol I is determined by the actual volume relaxation derived from the underlying large deformation. At lower elapsed time what appears as a strain softening is simply the result of the momentary rejuvenation, whose effects tend to vanish at longer times when the volume relaxations due to the large deformation actually brings it to completion.

The protocol type III is reported in Fig. 17. A large stress probe is inserted among the small ones. The small stress probes subsequent to the large one are used to "monitor" the material response to the large probe. Shortly after the large probe, Struik [1] observed an initial shifting of the creep behavior to shorter times followed by a shift of the response towards the one that would be expected had the large probe not been applied. This behavior is reported in Fig. 18.

This kind of behavior tried to be interpreted by neglecting the rejuvenation (i.e., the momentary interaction of structural

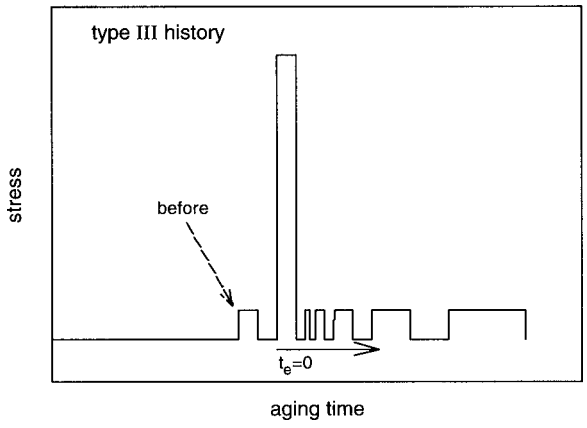

FIG. 17. Schematic of the protocol type III.

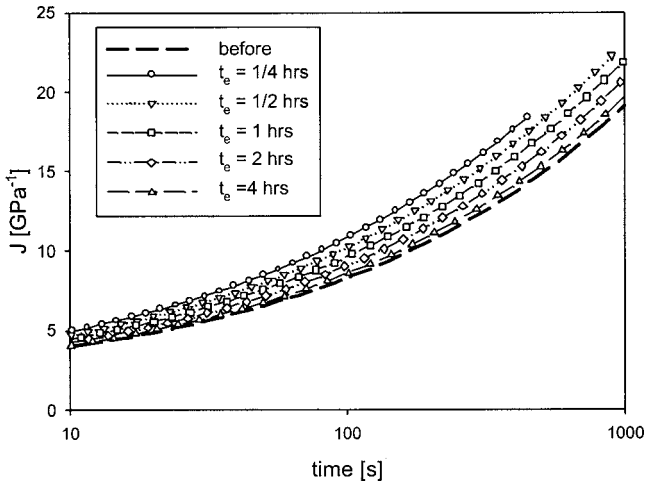

FIG. 18. Creep compliance before (dashed line) and after (symbols) the application of a large stress at different aging times measured from the application of the large stress (markers: simulations, lines: guides to eyes).

and stress relaxation phenomena). In doing so, the features of the viscoelastic response are attributed to the memory effects emerging inherently from the nonlinear viscoelastic materials behavior. However, using nonlinear viscoelastic models resulted in a qualitative description of the phenomena [15].

The simulations in terms of volume recovery behavior, illustrated in Fig. 19, allow a different description of the origin of the viscoelastic response. As expected, the ongoing volume relaxation derived from unloading the large stress is the real baseline supporting the responses to small stress probes: the momentary enhanced volume derived from the application of large stress shifts the viscoelastic response to shorter times with respect to the response obtained before it. Therefore, as time elapses and the volume relaxes toward the volume recovery baseline, the viscoelastic response at longer time tends to merge the response observed before the application of the large stress.

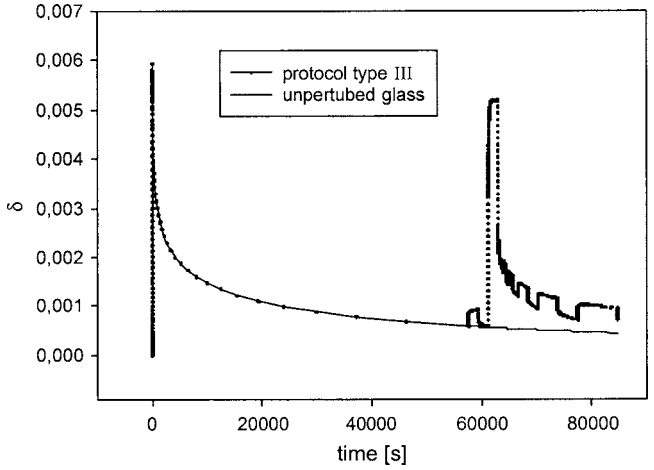

FIG. 19. Simulated volumetric response upon application of protocol III. The full line represents the unperturbed glass.

VI. CONCLUSIONS

A model describing the phenomenology of mechanically stimulated glass has been proposed. The development of the model is based on the simplest arguments conforming to the fundamentals of continuum mechanics from which a natural coupling of mechanical stress and volume recovery emerged. The simplest known formalism for viscoelastic relaxation was adopted while the well established KAHR phenomenological theory accounted for structural relaxation. The highly nonlinear phenomena were predicted assuming the simplest expression for the relaxation time (namely, the logarithm of relaxation time depends linearly on the temperature, the isotropic part of the stress tensor, and the dimensionless volume). The simulations of the volume as well as the viscoelastic response show qualitatively similar behavior (including the subtle features) as observed in the relevant results which appeared in literature over the years.

The concept of rejuvenation was clarified (it coincides substantially with the McKenna school of thought) explaining the occurrence of the time-aging time shift factors contraction. In all one can summarize that:

(a) Subyield mechanical perturbations do not alter the underlying structure of a glass as the volume recovery baseline remains unaltered.

(b) The *erasure of prior aging* by means of severe mechanical loadings is readily explained on the basis of the mutual influence of volume and mechanical relaxation. Higher stresses do not erase the previous aging (as reheating above T_g does). Aging simply reinitiates due to the effect of the stress on the actual volume of the glass.

(c) The effect of shift factors contraction is simply due to the volumetric creep debited to the isotropic part of the stress tensor. At higher stresses the (negative) effect of the underlying volume relaxation (that is irrespective of the actual stress) becomes less important. So that the momentary glass structures (i.e., the dimensionléss volumes) during adjacent tests are less different at higher stresses. Then the viscoelastic responses appear less shifted.

(d) Different loading conditions have been explored for the sake of proving the powerfulness of our model, plus additional knowledge derived from the volume recovery response concerning the protocols II and III.

(e) Based on general arguments derived from our simulations, the controversial density measurements resulting from post-yield stimulated glasses can be tentatively interpreted in terms of the time scales and the relative importance of the structural and the viscoelastic relaxations.

Finally, it is worth mentioning that the data reported by Struik, shows that the underlying phenomenology is identical under both tensile and torsion tests. However, the problem of torsional experiments on thick set samples requires further investigation because of the occurrence of a three-dimensional (3D) stress state. A 3D numerical procedure development is in progress in order to assess our model capabilities under the latter circumstances.

[1] L. C. E. Struik, *Physical Aging in Amorphous Polymers and Other Materials* (Elsevier, Amsterdam, 1978).
[2] G. Sherer, *Relaxation in Glass and Composites* (Wiley, New York, 1986).
[3] I. M. Hodge, J. Non-Cryst. Solids **169**, 211 (1994).
[4] C. A. Angell, K. L. Ngai, G. B. McKenna, P. F. McMillan, and S. W. Martin, J. Appl. Phys. **88**, 3113 (2000).
[5] J. M. Hutchinson, Prog. Polym. Sci. **20**, 703 (1995).
[6] S. S. Sternstein and T. C. Ho, J. Appl. Phys. **43**, 4370 (1972).
[7] G. B. McKenna and A. J. Kovacs, Polym. Eng. Sci. **24**, 1131 (1984).
[8] T. Ricco and T. L. Smith, Polymer **26**, 1979 (1985).
[9] G. B. McKenna and L. J. Zapas, J. Polym. Sci., Polym. Phys. Ed. **23**, 1647 (1985).
[10] G. B. McKenna and L. J. Zapas, Polym. Eng. Sci. **26**, 725 (1986).
[11] A. Lee and G. B. McKenna, Polymer **31**, 423 (1990).
[12] A. F. Yee, R. J. Bankert, K. L. Ngai, and R. W. Rendell, J. Polym. Sci., Part B: Polym. Phys. **26**, 2463 (1988).
[13] M. M. Santore, R. S. Duran, and G. B. McKenna, Polymer **32**, 2377 (1991).
[14] G. B. McKenna, J. Non-Cryst. Solids **172-174**, 756 (1994).
[15] W. K. Waldron, Jr., G. B. McKenna, and M. M. Santore, J. Rheol. **39**, 471 (1995).
[16] M. Delin, R. W. Rychwalski, J. Kubat, C. Klason, and J. M. Hutchinson, Polym. Eng. Sci. **36**, 2955 (1996).
[17] P. A. O'Connell and G. B. McKenna, Polym. Eng. Sci. **37**, 1485 (1997).
[18] G. B. McKenna, J. Phys.: Condens. Matter **15**, S737 (2003).
[19] J. M. Hutchinson, S. Smith, B. Horne, and G. M. Gourlay, Macromolecules **32**, 5046 (1999).
[20] M. L. Cerrada and G. B. McKenna, Macromolecules **33**, 3065 (2000).
[21] Y. Yang, A. D'Amore, Y. Di, L. Nicolais, and B. Li, J. Appl. Polym. Sci. **59**, 1159 (1996).
[22] B. E. Read, P. E. Tomlins, and G. D. Dean, Polymer **31**, 1204 (1990).
[23] L. C. E. Struik, Polymer **38**, 4053 (1997).
[24] S. L. Simon, J. Y. Park, and G. B. McKenna, Eur. Phys. J. E **E8**, 209 (2002).
[25] D. M. Colucci, G. B. McKenna, J. J. Filliben, A. Lee, D. B. Curliss, K. B. Bowman, and J. D. Russell, J. Polym. Sci., Part B: Polym. Phys. **35**, 1561 (1997).
[26] O. A. Hasan and M. C. Boyce, Polymer **34**, 5085 (1993).
[27] D. Cangialosi, M. Wübbenhorst, H. Schut, A. van Veen, and S. J. Picken, J. Chem. Phys. **122**, 064702 (2005).
[28] D. J. Lacks and M. J. Osborne, Phys. Rev. Lett. **93**, 255501 (2004).
[29] L. J. Broutman and R. S. Patil, Polym. Eng. Sci. **11**, 165 (1971).
[30] H. G. H. van Melic k, L. E. Govaert, B. Raas, W. J. Nauta, and H. E. H. Meijerm, Polymer **44**, 1171 (2003).
[31] G. Astarita, J. Rheol. **34**, 275 (1990).
[32] H. A. Barnes, J. Non-Newtonian Fluid Mech. **81**, 133 (1999).

[33] M. Ward and J. Sweeney, *An Introduction to the Mechanical Properties of Solid Polymers*, 2nd edition (John Wiley & Sons, New York, 2004).
[34] H. Leaderman, *Elastic and Creep Properties of Filamentous Materials and Other High Polymers* (Textile Foundation, Inc., Washington, D. C., 1943).
[35] M. L. Williams, R. F. Landel, and J. D. Ferry, J. Am. Chem. Soc. **77**, 3701 (1955).
[36] I. Emri and W. G. Knauss, Polym. Eng. Sci. **27**, 86 (1987).
[37] S. R. Lustig, R. M. Shay Jr., and J. M. Caruthers, J. Rheol. **40**, 69 (1996).
[38] J. M. Caruthers, D. B. Adolf, R. S. Chambers, and P. Shrikhande, Polymer **45**, 4577 (2004).
[39] D. B. Adolf, R. S. Chambers, and J. M. Caruthers, Polymer **45**, 4599 (2004).
[40] A. J. Kovacs, J. J. Aklonis, J. M. Hutchinson, and A. R. Ramos, J. Polym. Sci., Polym. Phys. Ed. **17**, 1097 (1979).
[41] A. R. Ramos *et al.*, J. Polym. Sci., Part B: Polym. Phys. **26**, 501 (1988).
[42] A. Q. Tool, J. Am. Ceram. Soc. **29**, 240 (1946).
[43] O. S. Narayanaswamy, J. Am. Ceram. Soc. **54**, 491 (1971).
[44] M. A. DeBolt, A. J. Easteal, P. B. Macedo, and C. T. Moynihan, J. Am. Ceram. Soc. **59**, 16 (1976).
[45] A. D'Amore, F. Caputo, L. Grassia, and M. Zarrelli, Composites, Part A **37**, 556 (2006).
[46] L. Grassia and A. D'Amore, Macromol. Symp. **228**, 1 (2005).